Preprints of the 21st IFAC World Congress (Virtual)
Berlin, Germany, July 12-17, 2020

A Frequency-shaped Controller for Damping Inter-area Oscillations in Power Systems ⋆

Felipe Wilches-Bernal * **David A. Schoenwald** *
Brian J. Pierre * **Raymond H. Byrne** *

* *Sandia National Laboratories, Albuquerque, NM 87185 USA (e-mail: {fwilche, daschoe, bjpierr, rhbyrne}@ sandia.gov).*

Abstract: This paper discusses how to design an inter-area oscillations damping controller using a frequency-shaped optimal output feedback control approach. This control approach was chosen because inter-area oscillations occur at a particular frequency range, from 0.2 to 1 Hz, which is the interval the control action must be prioritized. This paper shows that using only the filter for the system states can sufficiently damp the system modes. In addition, the paper shows that the filter for the input can be adjusted to provide primary frequency regulation to the system with no effect to the desired damping control action. Time domain simulations of a power system with a set of controllable power injection devices are presented to show the effectiveness of the designed controller.

Keywords: Damping control; inter-area oscillations; optimal control; frequency shaping; power systems stability; smart grids; small signal stability; primary frequency regulation

1. INTRODUCTION

Wide-area grids are systems with complex configurations of generation and load centers. These systems exhibit a phenomenon where power transfer between geographically separated areas have an oscillatory nature. These oscillations are the product of rotational speeds of groups of generators in one area oscillating against groups of generators in another area. The damping of these oscillations is affected by increases in power transfer between the areas and they are more prominent in sparsely interconnected systems, see Rogers (2012). Power grids worldwide are affected by this phenomenon; for the North American Eastern and Western interconnections refer, respectively, to Cui et al. (2017) and Ye et al. (2011), for the continental European interconnection (UCTE) see ENTSOE-E subgroup System Protection and Dynamics (2017).

Secure operations of power systems require inter-area oscillations to be damped at all times. Failure to take appropriate actions can lead to serious consequences such as the 1996 breakup of the North American Western Interconnection, see Kosterev et al. (1999). The damping of inter-area oscillations is typically done with devices known as power system stabilizers (PSSs). These devices act on the voltage control of conventional generators and generally use local information, see PSS (2007). Synchrophasor technology has made available time synchronized remote information for control design. For PSSs remote information can be helpful to their damping control action, see Chow et al. (2000). Remote information has also been instrumental to enabling other actuators such as HVDC lines for inter-area oscillation damping, see Schoenwald et al. (2017). From a control theory perspective, inter-area oscillations damping is a MIMO stability problem. Different control strategies such as optimal control and model predictive control have been used to approach this problem, see Wu et al. (2015); Chakrabortty (2012); Azad et al. (2013); Wilches-Bernal et al. (2018).

This paper uses a frequency-shaping optimal control approach to design a controller for damping inter-area oscillations in a two-area test power system. A set of controllable power injection devices is installed in the power system to be the actuators to provide the damping action. The frequency-shaping optimal control approach, advanced in the works of Moore and Mingori (1987); Khorrami and Ozguner (1988); Hu et al. (1990); Mourad et al. (2012), was selected because of the nature of inter-area oscillations: a phenomenon that occurs at a narrow and defined frequency range. Hence, the designed controller is focused to mainly act within this frequency interval. Because the paper aims at a realistic scenario, the control action is restricted to using only machine speeds as available information. For this reason, the problem is approached as an optimal output feedback control problem. The paper shows the conditions to solve a frequency-shaping optimal output feedback control problem and uses them to design an inter-area oscillations damping controller. Because a frequency-shaping optimal controller requires two filters, one to penalize the *states*, and another to penalize the inputs, the paper shows how they affect the control action and the overall response of the system. In particular, it is

⋆ Sandia National Laboratories is a multimission laboratory managed and operated by National Technology and Engineering Solutions of Sandia, LLC., a wholly owned subsidiary of Honeywell International, Inc., for the U.S. Department of Energy's National Nuclear Security Administration under contract DE-NA0003525. This research was supported by the U.S. Department of Energy Transmission Reliability program.

shown that the filter for the states is the only filter necessary to provide sufficient inter-area oscillations damping to the system. The inclusion of a filter for the inputs is shown to be effective at improving the primary frequency regulation of the system while not affecting the damping action. Time domain simulations of the test system for a power imbalance event are presented to demonstrate the effectiveness of the designed controller.

The rest of the paper is organized as follows. Section 2 elaborates the theory of frequency-shaping optimal output feedback control. Section 3 presents the test system and the design of the filters. Section 4 presents time domain simulations testing the proposed controllers. Finally, Section 5 discusses the conclusions and future work of the research presented here.

2. FREQUENCY SHAPING OPTIMAL CONTROL

The state-space representation of a linear time invariant system is

$$\dot{x}(t) = Ax(t) + Bu(t) \tag{1}$$
$$y(t) = Cx(t) \tag{2}$$

where $x \in \mathbb{R}^n$, $u \in \mathbb{R}^m$, and $y \in \mathbb{R}^p$, respectively, are the state, the control input, and the system output. The standard linear-quadratic regulator (LQR) for infinite horizon is obtained by obtaining the input u that minimizes the cost function

$$J(u) = \int_0^\infty \left(x(t)^\top Q x(t) + u(t)^\top R u(t)\right) dt \tag{3}$$

where $Q \geq 0 \ \in \mathbb{R}^{n\times n}$ and $R > 0 \ \in \mathbb{R}^{n\times n}$ are matrices to penalize, respectively, the states of the system and the control effort. Using Parseval's theorem the cost in (3) can be rewritten in frequency domain as

$$J(u) = \frac{1}{2\pi}\int_0^\infty \left(X(j\omega)^{\mathsf{H}} Q X(j\omega) + U(j\omega)^{\mathsf{H}} R U(j\omega)\right) d\omega \tag{4}$$

Matrices Q and R can be made frequency dependent as

$$Q(j\omega) = Q_{\mathrm{f}}(j\omega)^{\mathsf{H}} Q_{\mathrm{f}}(j\omega) \succeq 0 \tag{5}$$
$$R(j\omega) = R_{\mathrm{g}}(j\omega)^{\mathsf{H}} R_{\mathrm{g}}(j\omega) \succ 0 \tag{6}$$

By defining a filtered version of the state and the input as

$$X_{\mathrm{f}}(j\omega) = Q_{\mathrm{f}}(j\omega)X(j\omega) \tag{7}$$
$$U_{\mathrm{g}}(j\omega) = R_{\mathrm{g}}(j\omega)U(j\omega) \tag{8}$$

the frequency domain cost function in (4) can be rewritten as

$$J(u) = \frac{1}{2\pi}\int_0^\infty \left(X_{\mathrm{f}}(j\omega)^{\mathsf{H}} X_{\mathrm{f}}(j\omega) + U_{\mathrm{g}}(j\omega)^{\mathsf{H}} U_{\mathrm{g}}(j\omega)\right) d\omega \tag{9}$$

and its time domain equivalent as

$$J(u) = \int_0^\infty \left(x_{\mathrm{f}}(t)^\top x_{\mathrm{f}}(t) + u_{\mathrm{g}}(t)^\top u_{\mathrm{g}}(t)\right) dt \tag{10}$$

The state space representation of the filter Q_f with input $x(t)$ and output $x_{\mathrm{f}}(t)$ is

$$\dot{z}_Q(t) = A_Q z_Q(t) + B_Q x(t) \tag{11}$$
$$x_{\mathrm{f}}(t) = C_Q z_Q(t) + D_Q x(t) \tag{12}$$

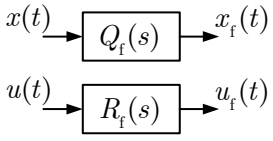

Fig. 1. Filtered signals.

where $z_Q \in \mathbb{R}^{n_Q}$ and $x_{\mathrm{f}} \in \mathbb{R}^{n_f}$. Similarly, the state space representation of the filter R_f with input $u(t)$ and output $u_{\mathrm{f}}(t)$ is

$$\dot{z}_R(t) = A_R z_Q(t) + B_R u(t) \tag{13}$$
$$u_{\mathrm{f}}(t) = C_R z_R(t) + D_R u(t) \tag{14}$$

where $z_R \in \mathbb{R}^{n_R}$ and $u_{\mathrm{g}} \in \mathbb{R}^{n_g}$. Using the filters for both the input and the states, an extended state space representation can be formulated as

$$\underbrace{\begin{bmatrix}\dot{x}(t)\\ \dot{z}_Q(t)\\ \dot{z}_R(t)\end{bmatrix}}_{\dot{x}_{\mathrm{e}}} = \underbrace{\begin{bmatrix}A & 0 & 0\\ B_Q & A_Q & 0\\ 0 & 0 & A_R\end{bmatrix}}_{A_{\mathrm{e}}} \underbrace{\begin{bmatrix}x(t)\\ z_Q(t)\\ z_R(t)\end{bmatrix}}_{x_{\mathrm{e}}} + \underbrace{\begin{bmatrix}B\\ 0\\ B_R\end{bmatrix}}_{B_{\mathrm{e}}} u(t) \tag{15}$$

In this new representation, the cost function is

$$J(u) = \int_0^\infty \Big(x_{\mathrm{e}}(t)^\top Q_{\mathrm{e}} x_{\mathrm{e}}(t) + 2u(t)^\top N_{\mathrm{e}} x_{\mathrm{e}}(t) + u(t)^\top R_{\mathrm{e}} u(t)\Big) dt \tag{16}$$

where Q_e, N_e and R_e are defined below

$$Q_{\mathrm{e}} = \begin{bmatrix} D_Q^\top D_Q & D_Q^\top C_Q & 0\\ C_Q^\top D_Q & C_Q^\top C_Q & 0\\ 0 & 0 & C_R^\top C_R\end{bmatrix} \tag{17}$$
$$N_{\mathrm{e}} = \begin{bmatrix}0 & 0 & D_R^\top C_R\end{bmatrix} \tag{18}$$
$$R_{\mathrm{e}} = D_R^\top D_R \tag{19}$$

The solution to this system can be found using the following Riccati equation

$$A_{\mathrm{e}}P_{\mathrm{e}} + P_{\mathrm{e}}A_{\mathrm{e}} - (B_{\mathrm{e}}^\top P_{\mathrm{e}} + N_{\mathrm{e}})^\top R_{\mathrm{e}}^{-1}(B_{\mathrm{e}}^\top P_{\mathrm{e}} + N_{\mathrm{e}}) + Q_{\mathrm{e}} = 0 \tag{20}$$

and the optimal input to the system is then

$$u_{\mathrm{opt}}(t) = -R_{\mathrm{e}}^{-1}(B_{\mathrm{e}}^\top P_{\mathrm{e}} + N_{\mathrm{e}})x_{\mathrm{e}}(t) \tag{21}$$

Assuming the only accessible variables for control design are the output variables of the system and the filter signals then

$$y_{\mathrm{e}}(t) = C_{\mathrm{e}}x_{\mathrm{e}}(t) + D_{\mathrm{e}}u(t) \tag{22}$$

with

$$C_{\mathrm{e}} = \begin{bmatrix}C & 0 & 0\\ 0 & I_{n_Q} & 0\\ 0 & 0 & I_{n_R}\end{bmatrix} \qquad D_e = \begin{bmatrix}D\\ 0\\ 0\end{bmatrix} \tag{23}$$

where C_{e} has $p+n_Q+n_R$ rows and $n+n_Q+n_R$ columns. If a constraint is included where the control law can only use information from the outputs as

$$u(t) = K y_{\mathrm{e}}(t) \tag{24}$$

then a frequency-shaping optimal output feedback control is determined by

$$K = -R_{\mathrm{e}}^{-1}(B_{\mathrm{e}}^\top P + N_{\mathrm{e}})\Lambda C_{\mathrm{e}}^\top (C_{\mathrm{e}}\Lambda C_{\mathrm{e}}^\top)^{-1} \tag{25}$$
$$0 = Q_{\mathrm{e}} + C_{\mathrm{e}}^\top K^\top N_{\mathrm{e}} + N_{\mathrm{e}}^\top K C_{\mathrm{e}} + C_{\mathrm{e}}^\top K^\top R_{\mathrm{e}} K C_{\mathrm{e}} + P(A_{\mathrm{e}} + B_{\mathrm{e}}KC_{\mathrm{e}}) + (A_{\mathrm{e}} + B_{\mathrm{e}}KC_{\mathrm{e}})^\top P \tag{26}$$
$$0 = (A_{\mathrm{e}} + B_{\mathrm{e}}KC_{\mathrm{e}})\Lambda + \Lambda(A_{\mathrm{e}} + B_{\mathrm{e}}KC_{\mathrm{e}})^\top + X_0 \tag{27}$$

where X_0 is the expected value of the initial conditions of the states. The solution of the system of matrix equations (25)-(27) determines the gain of the frequency-shaping optimal output feedback control problem. These set of equations can be solved by an iterative procedure such as Algorithm 1 shown below. Note that Algorithm 1 is an Anderson-Moore type of algorithm; for information about its properties and convergence see Rautert and Sachs (1997).

Algorithm 1:

1. Select a stabilizing control gain $K_k = K_0$ so that $A_e + B_e K_0 C_e$ is stable. Set $K = 0$ and choose a positive number for parameter δ that is small according to the application.
2. Setting $K = K_k$ solve the Lyapunov equation (27) for $\Lambda \to \Lambda_k$
3. Setting $K = K_k$ solve the Lyapunov equation (26) for $P \to P_k$
4. With Λ and P obtained from the two steps above, compute the optimal gain, $K \to K_k$, using relationship (25)
5. Compute the descent direction $\Delta K_k = \hat{K}_k - K_k$.
6. Compute the Frobenius norm of the descent as $\|\Delta K_k\|_F$. If $\|\Delta K_k\|_F \leq \delta$, stop the algorithm; otherwise, choose a value of α_k, between 0 and 1 and update the gain by computing

$$K_{k+1} = K_k + \alpha \Delta K_k$$

set $k = k + 1$, and go to Step 2.

3. CONTROLLER DESIGN

This section introduces a test power system that has poorly damped inter-area oscillations and the filters Q_f and R_g selected to damp these oscillations.

3.1 Test Power System

The test power system used in this work is shown in Fig. 2. This is a widely used model in the power system community as it exhibits a dominant inter-area oscillation, see Kundur (1994); Klein et al. (1991). The system has 4 synchronous generators and two loads in two areas connected by two transmission lines. The inter-area oscillation has generators in Area 1, G1 and G2, oscillating against generators in Area 2, G2 and G4; its damping can be modified by the power transfer between the areas: the more power is transferred from one area to another the less damping the system has. This system was modified to include 6 controllable power injection devices: ES1, ES2, ES3 in Area 1, and ES4, ES5, ES6 in Area 2. An example of such devices is power electronic interfaced energy storage. The operating condition selected for the system has all the generators producing around 700 MW and Area 1 is exporting around 100 MW to Area 2. The main inter-area mode is at $-0.221 \pm j3.435$ with a damping of 2.8% and a frequency around 0.55 Hz.

The aim of this work is to design a controller for the power injection devices to damp the oscillations of the system in Fig. 2 using the frequency-shaping optimal control approach described in Section 2. A state-space representation, such as (1), of the power system is necessary. The tool used to represent the system and obtain its linearized version is the Power System Toolbox (PST) described in Chow and Cheung (1992); Wilches-Bernal et al. (2014). The linearized system has $x \in \mathbb{R}^{28}$, $u \in \mathbb{R}^6$, $y \in \mathbb{R}^4$. The outputs, y, are the machine speeds of the generators and the inputs, u, are the active power injections of the power injection devices. The availability of only the machine speeds is a realistic assumptions for power systems and as such the control problem is an optimal output feedback control where the optimal gain can only make use of the outputs as $u_{\text{opt}}(t) = Ky(t)$.

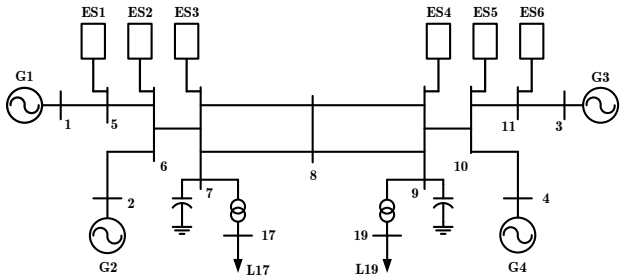

Fig. 2. Two-area power system with six controllable power injection devices, three per area.

3.2 Filter Design

Power system inter-area oscillations are generally found in the frequency interval between 0.2 and 1 Hz, see Kundur (1994); Rogers (2012). The filters selected for the frequency-shaping control should be such that they emphasize this frequency range. The filter Q_f was selected to be of the following form

$$Q_f(s) = q_f(s) I_p C \tag{28}$$

where I_p is an identity matrix of dimension p and the output matrix C was used to reflect that only the system outputs are available. $q(s)$ is selected to be a fourth order Bessel filter of the form

$$q_f(s) = \frac{\gamma_Q a s^2}{s^4 + b_3 s^3 + b_2 s^2 + b_1 s + b_0} \tag{29}$$

where $a = 75.18$, $b_0 = 50.5$, $b_1 = 106.7$, $b_2 = 89.39$, and $b_3 = 15.02$. γ_Q is a constant that determines the weight given to the state term in the cost function. The frequency response of $q_f(s)$ can be observed in Fig. 3. This filter has cutoff frequencies at 0.12 and 1.5 Hz.

The filter to the input signals is

$$R_f(s) = r_f(s) I_m \tag{30}$$

where I_m is an identity matrix of dimension m and $r_f(s)$ is a SISO filter. The basic form of $r_f(s)$ is

$$r_f(s) = \frac{\gamma_R (s - z_r)}{T_r s + 1} \tag{31}$$

where γ_R is a constant that determines the weight given to the term with the inputs in the cost function. This research explores the effects of different forms of $r_f(s)$ on the response of the system. Three different $r_f(s)$ filters were tested:

- No filter case. In this case $r_f(s) = \gamma_R$ and is not dependent on frequency.
- case where $z_r = 1$ and $T_r = 5$, named r_{f1}.

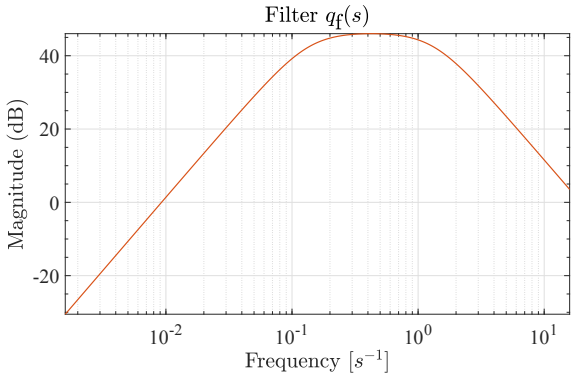

(a) Magnitude Bode Plot.

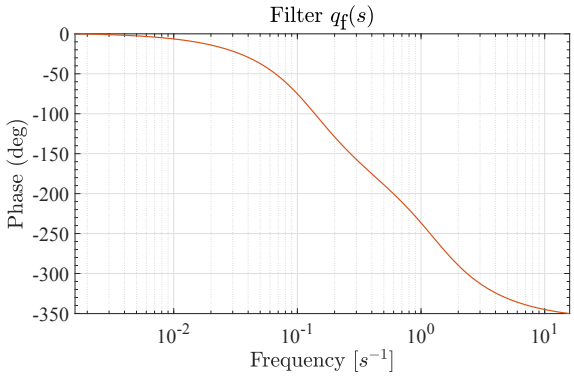

(b) Phase Bode Plot.

Fig. 3. Frequency response of the filter $q_f(s)$.

- case where $z_r = 1$ and $T_r = 20$, named r_{f2}.

The frequency response of the different cases for $r_f(s)$ are observed in Fig 4.

4. RESULTS

This section presents results of using the controllers presented in Section 3 to damp the inter-area oscillations of the system in Fig. 2.

Fig. 5 shows the eigenvalues of the test power system. The blue '×'-markers show the eigenvalues for the uncontrolled system. The red stars show the eigenvalues of the system with the frequency shaping controller when $r_f(s) = \gamma_R$; an input filter that is not dependent on frequency. The yellow '+'-markers and the purple diamond-shaped markers show the eigenvalues when the input filter corresponds to $r_{f1}(s)$ and $r_{f2}(s)$, respectively. The results in this figure clearly show that the eigenvalues of the uncontrolled system moved towards stability i.e. the left-hand plane when control is added.

Time domain simulations were carried out to validate the results presented and show how the controllers damp the oscillations in the system. The simulations were performed in PST. The event considered was the increase of the load at Bus 17. The operating condition of this load is to consume 12.67 pu of power which was increased by 1 pu after one second following the start of the simulation.

Fig. 6a shows the difference of machine speeds between G3, a generator in Area 2, and G1, a generator in Area 1 while fig. 6a shows the difference of machine speeds

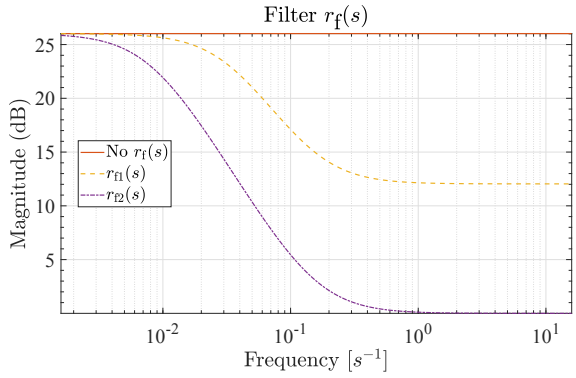

(a) Magnitude Bode Plot.

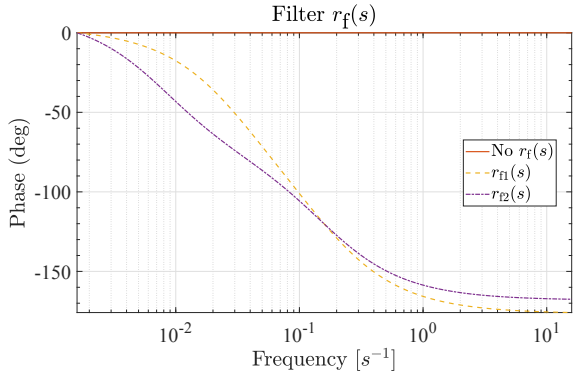

(b) Phase Bode Plot.

Fig. 4. Frequency response of the filter for the inputs (R).

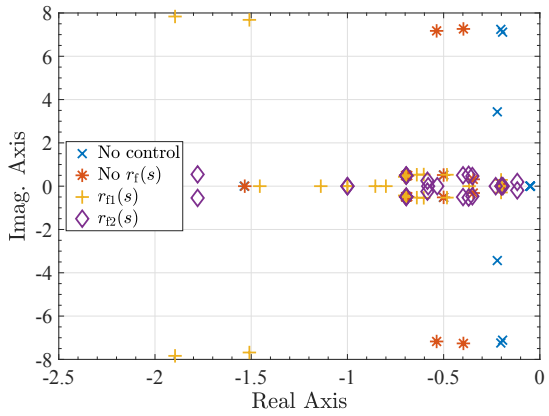

Fig. 5. Eigenvalues of the system in Fig. 2 in open and in closed loop.

between G4, a generator in Area 2, and G2, a generator in Area 1. Frequency differences are shown because they clearly exhibit the inter-area oscillations of the system. These figures show results for the four following cases: the no control case in blue lines; the case where $r_f(s)$ is not dependent on frequency in red; the case with $r_{f1}(s)$ as input filter in yellow; and the case using $r_{f2}(s)$ in purple. The results in these two figures show that the uncontrolled system has a poorly damped oscillation around 0.55 Hz (the frequency of the inter-area mode) which are only fully damped after 20 seconds from the start of the disturbance. The results for all the cases where a controller is included show that inter-area oscillations are rapidly damped and they disappear approximately 6 seconds after the load was connected. The results in Fig. 6a with the frequency

difference between G1 and G3 show that the amplitude of the first swing of the oscillations has been reduced from roughly 0.1 Hz in the uncontrolled case to approximately 0.03 Hz for the $r_{\mathrm{f}} = \gamma_R$ case. Similarly, fig. 6b with results for the frequency difference between G4 and G2, show a first swing amplitude reduction from about 0.1 Hz in the uncontrolled case to around 0.06 Hz for all the cases with control.

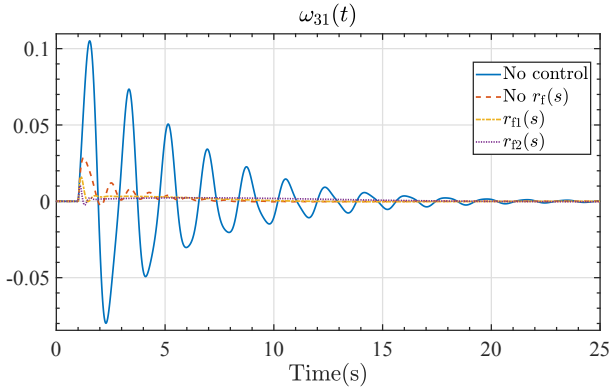

(a) Machine speed difference between Gens 3 and 1.

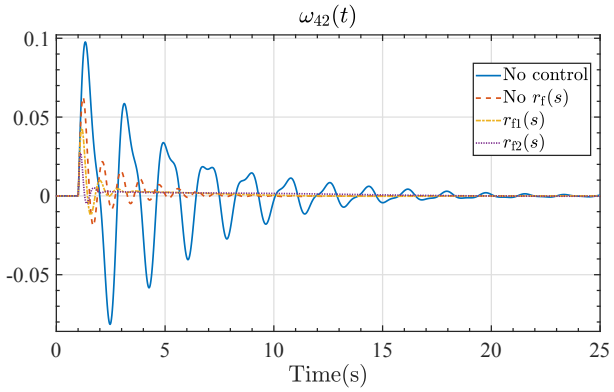

(b) Machine speed difference between Gens 4 and 2.

Fig. 6. Machine speed difference between Gens 3 and 1, and Gens 4 and 2 for the cases with and without the frequency shaping controller.

Fig. 7 shows the machine speed of G1 and G3 for the event described above for the same four cases as those in Fig. 6. The results show that the machine speeds for the uncontrolled case exhibit an inter-area oscillation in addition to the typical shape obtained for power shortage events. This shape is of a curve with a *rapid* decrease of frequency (or machine speed) before a nadir is reached after which the frequency starts increasing, due to governor action, at a slower rate to reach a settling point which is still lower than the nominal value. This shape represents the primary frequency regulation of the system and is similar for the speeds of all machines in the system (with the main differences among them stemming from inter-area oscillations or local phenomena). The results in Fig. 7a show all the control cases are able to damp the inter-area oscillations and are in line with those in Fig. 6. These results also show that the effect of the controller, $r_{\mathrm{f}} = \gamma_R$, is primarily to damp inter-area oscillations without affecting the primary frequency regulation of the system. The results in Fig. 7 also show that including an input filter, as was done for the $r_{\mathrm{f1}}(s)$ and $r_{\mathrm{f2}}(s)$ cases, heavily affects the primary frequency regulation of the system. The yellow lines when the filter is $r_{\mathrm{f1}}(s)$ show that the frequency nadir of the system is improved with respect to the non control case. The results when the filter is $r_{\mathrm{f2}}(s)$, in purple lines, show this filter significantly improves the frequency nadir and the overall primary frequency response of the system. The results also show that the settling frequency is almost unaffected by any of the filters.

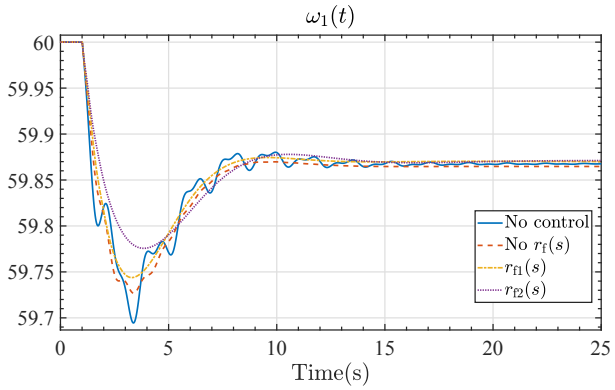

(a) Machine speed of Gen 1.

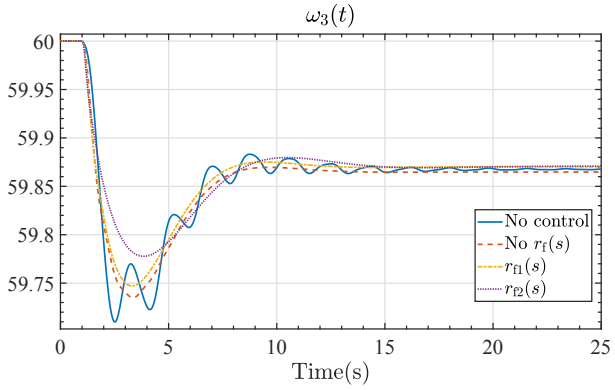

(b) Machine speed of Gen 3.

Fig. 7. Machine speeds of Gens 1 and 3 with and without the frequency shaping controller.

Figs. 8a and 8b show, respectively, the power injection action of ES1 and ES4 to achieve the small-signal stability and primary frequency regulation improvements shown in Figs. 7 and 6 for all the control cases considered. The results in these figures show that the action of the power injection devices last longer for the input filter $r_{\mathrm{f1}}(s)$ and $r_{\mathrm{f2}}(s)$ cases. This is the result of their action to help with the primary frequency regulation of the system.

5. CONCLUSIONS AND FUTURE WORK

This paper presents the design of a controller to damp inter-area oscillations in a test power system with controllable power injection devices. The controller is based on the frequency-shaping optimal output feedback control approach that assumes the only outputs available are the generator rotational speeds. The paper presents the frequency-shaping optimal control preliminaries and the modifications needed when an additional constraint for the optimal gain to only use available outputs is included. The paper shows how to carefully design the filter for the state signals to emphasize the 0.2 to 1 Hz frequency interval

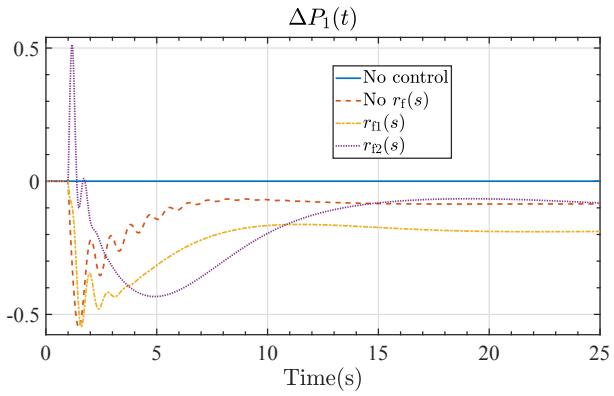

(a) Power injection of ES1.

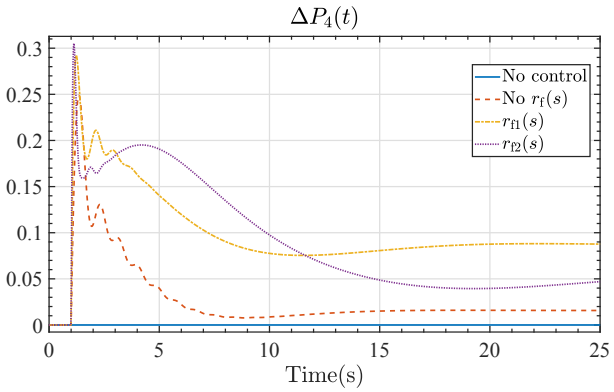

(b) Power injection of ES4.

Fig. 8. Power injections of ES1 and ES4 with and without the frequency shaping controller.

where inter-area oscillations occur. Time-domain simulations in a power system with poorly damped oscillations show that the proposed controller is able to effectively damp them. Additionally, the paper analyzes how the filter for the inputs in the frequency-shaping approach is able to modify the primary frequency regulation of the system while retaining the damping capability of the controller and without affecting the steady-state response of the system.

Future work will extend this approach to larger power systems and consider the modulation of both active and reactive power of the actuators.

REFERENCES

(2007). *IEEE Tutorial Course - Power System Stabilization via Excitation Control*. IEEE Power & Energy Soc., Piscataway, NJ.

Azad, S.P., Iravani, R., and Tate, J.E. (2013). Damping inter-area oscillations based on a model predictive control (mpc) hvdc supplementary controller. *IEEE Transactions on Power Systems*, 28(3), 3174–3183.

Chakrabortty, A. (2012). Wide-area damping control of power systems using dynamic clustering and TCSC-based redesigns. *IEEE Trans. Smart Grid*, 3(3), 1503–1514.

Chow, J.H. and Cheung, K.W. (1992). A toolbox for power system dynamics and control engineering education and research. *IEEE Trans. Power Syst.*, 7(4), 1559–1564.

Chow, J.H., Sanchez-Gasca, J.J., Ren, H., and Wang, S. (2000). Power system damping controller design using multiple input signals. *IEEE Control Syst. Mag.*, 20(4), 82–90.

Cui, Y., Wu, L., Yu, W., Liu, Y., Yao, W., Zhou, D., and Liu, Y. (2017). Inter-area oscillation statistical analysis of the us eastern interconnection. *The Journal of Engineering*, 2017(11), 595–605.

ENTSOE-E sub-group System Protection and Dynamics (2017). Analysis of ce inter-area oscillations of 1st december 2016. Technical report, ENTSO-E, Brussels, Belgium.

Hu, H.X., Loh, N., and Cheok, K. (1990). Frequency-shaping optimal parameteric lq control with application. In *[Proceedings] IECON'90: 16th Annual Conference of IEEE Industrial Electronics Society*, 142–147. IEEE.

Khorrami, F. and Ozguner, U. (1988). Frequency-shaped cost functionals for decentralized systems. In *Proceedings of the 27th IEEE Conference on Decision and Control*, 417–422. IEEE.

Klein, M., Rogers, G.J., and Kundur, P. (1991). A fundamental study of inter-area oscillations in power systems. *IEEE Trans. Power Syst.*, 6(3), 914–921.

Kosterev, D.N., Taylor, C.W., and Mittelstadt, W. (1999). Model validation for the August 10, 1996 WSCC system outage. *IEEE Trans. Power Syst.*, 14(3), 967–979.

Kundur, P. (1994). *Power System Stability and Control*. McGraw-Hill, New York, NY.

Moore, J.B. and Mingori, D.L. (1987). Robust frequency-shaped lq control. *Automatica*, 23(5), 641–646.

Mourad, L., Claveau, F., and Chevrel, P. (2012). Design of a two DOF gain scheduled frequency shaped LQ controller for narrow tilting vehicles. In *2012 American control conference (ACC)*, 6739–6744. IEEE.

Rautert, T. and Sachs, E.W. (1997). Computational design of optimal output feedback controllers. *SIAM Journal on Optimization*, 7(3), 837–852.

Rogers, G. (2012). *Power system oscillations*. Springer Science & Business Media.

Schoenwald, D.A., Pierre, B.J., Wilches-Bernal, F., and Trudnowski, D.J. (2017). Design and implementation of a wide-area damping controller using high voltage dc modulation and synchrophasor feedback. *IFAC-PapersOnLine*, 50(1), 67–72.

Wilches-Bernal, F., Copp, D.A., Bacelli, G., and Byrne, R.H. (2018). Structuring the optimal output feedback control gain: A soft constraint approach. In *2018 IEEE Conference on Decision and Control (CDC)*, 2464–2469. IEEE.

Wilches-Bernal, F., Sanchez-Gasca, J.J., and Chow, J.H. (2014). Implementation of wind turbine generator models in the power system toolbox. In *2014 Power and Energy Conference at Illinois (PECI)*, 1–5. IEEE.

Wu, X., Dörfler, F., and Jovanović, M.R. (2015). Decentralized optimal control of inter-area oscillations in bulk power systems. In *2015 54th IEEE Conference on Decision and Control (CDC)*, 5532–5537. IEEE.

Ye, Y., Gardner, R.M., and Liu, Y. (2011). Oscillation analysis in western interconnection using distribution-level phasor measurements. In *2011 IEEE Power and Energy Society General Meeting*, 1–8. IEEE.